Available online at www.sciencedirect.com
ScienceDirect
Ceramics International 34 (2008) 125–130
CERAMICS INTERNATIONAL
www.elsevier.com/locate/ceramint

Preparation of glass-ceramics from red mud in the aluminium industries

Jiakuan Yang [a,b,*], Dudu Zhang [a], Jian Hou [b], Baoping He [a], Bo Xiao [a]

[a] College of Environmental Science and Engineering, Huazhong University of Science & Technology, Wuhan, Hubei 430074, China
[b] Shandong Aluminium Co. Ltd., Zibo, Shandong 255100, China

Received 5 April 2006; received in revised form 5 June 2006; accepted 22 August 2006
Available online 1 November 2006

Abstract

The feasibility of recycling red mud and fly ash in the aluminium industries by producing glasses and glass-ceramics has been investigated. The crystallization behavior of glass-ceramics mostly produced from red mud and fly ash was studied by DTA, XRD, optical microscopy techniques. According to DTA curve, nucleation experiments were carried out at various nucleation temperatures at the same crystallization temperature of 900 °C for 2 h, and crystallization experiments were performed at the same nucleation temperature of 697 °C for 2 h followed by crystallization at various temperatures. The nucleation results show that optimum nucleation temperature is near 697 °C, and the crystallization experiments show that the crystallization at a high temperature of over 900 °C results in denser grain size. The major crystallized phases were gehlenite ($Ca_2Al_2SiO_7$), and augite ($Ca(Fe,Mg)Si_2O_6$). The XRD results show that with the increase of crystallization temperature, the amount of gehlenite increases, and augite decreases, which is the result of augite transformation into gehlenite.

Keywords: Glass-ceramics; Red mud; Fly ash; Crystallization; Verification; Wastes recovery

1. Introduction

Red mud is the solid waste residue from the caustic soda leaching of bauxite ores to produce alumina, and its major constituents are CaO, Al_2O_3, SiO_2, Na_2O, TiO_2 and Fe_2O_3, with little amounts of Ga, V, Sr, Zr, Y, Th, U and rare earth elements as trace constituents. Production of 1 t of alumina is accompanied by generation of about 1.0–1.5 t of red mud. It is estimated that over 66 million tonnes of this waste is impounded annually in the world, with 2 million tonnes in India [1]. There were nearly 3 million tonnes of red mud wastes accumulated at an aluminium plant in Turkey between 1973 and 1996 [2]. Chinese alumina plants generate 3.8–4.0 million tonnes of red mud wastes accompanied with the consumption of 6 million tonnes bauxite ores every year [3]. Shandong Aluminium Co. Ltd. (formerly called Shandong Aluminium Plant), one of the subsidiary companies of Aluminium Corporation of China Limited, is the first aluminium plant in China, located in Zibo that is a ceramic hometown in China. There have been more than 22 million tonnes of red mud wastes accumulated at Shandong Aluminium Plant since the plant was setup in 1954. The old landfill site of red mud occupies the land of 700 m × 800 m, at the height of over 70 m, reaching the capacity limit. In 2001, the new landfill was constructed for disposal of red mud wastes, about 1 million tonnes every year, and total amount of investment was more than 70 million yuans, most of which was spent on the construction of the geomembrane liner system for preventing the alkaline from leaching into underground water. It is more than a century that industry has not come up with any viable alternate economic method to treat bauxite for production alumina, which does not generate red mud.

The disposal of such a large quantity of red mud slurry retaining variable water content is expensive (up to 1–2% of the alumina price), presents serious problems of storing, and causes environmental pollution. Although studies in this area have been done for 40–50 years of R&D efforts, effective reuse technologies have mostly not been put into practice because of economic reasons, and no significant quantity of red mud is actually being utilized anywhere in the world.

During the last two decades, extensive work has been done to develop various processes for utilization of red mud by the researchers in the various areas. Singh et al. prepared special

* Corresponding author at: College of Environmental Science and Engineering, Huazhong University of Science & Technology, Wuhan, Hubei 430074, China. Tel.: +86 27 877 92207; fax: +86 27 875 43512.
E-mail address: yjiakuan@hotmail.com (J. Yang).

0272-8842/$32.00
doi:10.1016/j.ceramint.2006.08.013

cements from red mud [4]. Sglavo et al. developed use of red mud in the ceramic industry [5]. Yalçin and Sevinç studied on bauxite waste in ceramic glazes [2]. Şayan and Bayramoğlu studied the recovery with sulfuric acid leaching of Ti content of red mud [6], a waste of Turkey Etibank Seydişehir Aluminium plants.

In 2003, Aluminium Corporation of China Limited funded the research project to recovery the red mud in Shandong Aluminium Co. Ltd. This research work has been carried out by both Huazhong University of Science & Technology and Research Institute of Shandong Aluminium Co. Ltd. to develop different processes for utilization of red mud. Three main applications that have been investigated include: (i) production of non-fired construction bricks [7], (ii) development of road materials [8], (iii) preparation of glass-ceramics. Since the use of industrial solid wastes for production of slag-based glass-ceramics has many commercial applications, the transformation of waste into glass or glass-ceramics provided the opportunity for making useful, and marketable products [9,10], like interior claddings, roof coverings, water-permeable blocks, pavement bricks. There have been many research works of glass-ceramics based on slag, such as blast furnace slag, steel slag, MSW incineration fly ash, coal combustion fly ash, sewage sludge [11–16]. However, less research has been reported on glass-ceramics made from red mud.

In this paper, glass-ceramics are prepared from red mud in the aluminium industry and fly ash in the coal-combustion power plant, and the crystalline phases, microstructure of the materials have been studied.

2. Experimental

2.1. Raw materials and glass-ceramic forming

The red mud sample was supplied by Shandong Aluminium Co. Ltd. The red mud powder sample was ground after dried at 105 °C for 10 h, for removal of the retained variable water in the red mud. The chemical compositions of red mud powder sample are shown as Table 1. The red mud is CaO-rich slag from the Sintering process in Shandong Aluminium Co. Ltd. In order to design the $CaO–Al_2O_3–SiO_2$ glass-ceramics system, SiO_2-rich, and Al_2O_3-rich raw materials are suggested to be added, so dry fly ash, a cheap and convenient SiO_2-rich, and Al_2O_3-rich waste directly collected from electrostatic precipitator in the coal-combustion power plant, is another main raw material, with addition of a small amount of silica sand powder. The chemical compositions of dry fly ash and silica sand powder are also reported in Table 1. The TiO_2 of chemical grade was added as nucleation agent, and Na_2CO_3 was added to improve the ability of glass forming. The composition of parent glass samples are reported in Table 2.

Table 2
Composition of parent glass sample

Amount of raw materials (wt%)	
Red mud	52
Fly ash	33
Silica sand	9
TiO_2	1
Na_2CO_3	5
Calculated composition of parent glass (wt%)	
SiO_2	38.01
CaO	26.97
Al_2O_3	16.46
Fe_2O_3	9.56
MgO	1.20
Na_2O	4.82
K_2O	0.61
TiO_2	2.38

After grinding, the mixed powders were melted in air using Al_2O_3 crucible at 1360 °C, then the melt was cast in preheated steel moulds. To remove thermal residual stresses, the as-cast glass samples were annealed in the muffle, followed by slow cooling to the room temperature.

2.2. Differential thermal analysis (DTA)

Crystallization process was investigated by DTA technique (Perkin-Elmer 7 Series Thermal Analyzer), using 30.300 mg powder glass samples heated from 20 to 1200 °C at a rate of 10 °C/min. DTA was carried to determine the glass transition temperature (T_g) and crystallization peak temperature (T_p).

2.3. Thermal treatments

On the basis of DTA analyses, nucleation experiments were conducted at temperatures in the range of 650–720 °C, near the glass transition temperature (T_g), at the holding time of 2 h. Following nucleation, the temperature was raised to the desired crystallization temperature in the range of 850–1200 °C, near crystallization peak temperature (T_p), and held for 2 h followed by air cooling. The rationale for choosing the optimum heat-treatment conditions is explained in the following discussion section.

2.4. Microstructure characterization

Microstructure characterization experiments of glass-ceramic at the different heat-treatment conditions were performed

Table 1
Compositions of main raw materials (wt%)

Raw materials	SiO_2	CaO	Al_2O_3	Fe_2O_3	MgO	Na_2O	K_2O	TiO_2	LOI
Red mud	18.10	42.21	7.02	13.69	2.06	2.38	0.24	2.10	12.20
Fly ash	49.44	6.60	33.34	4.23	0	0.51	1.28	0	4.60
Silica sand	93.42	1.02	1.44	0.83	0.07	0	0	0.47	2.75

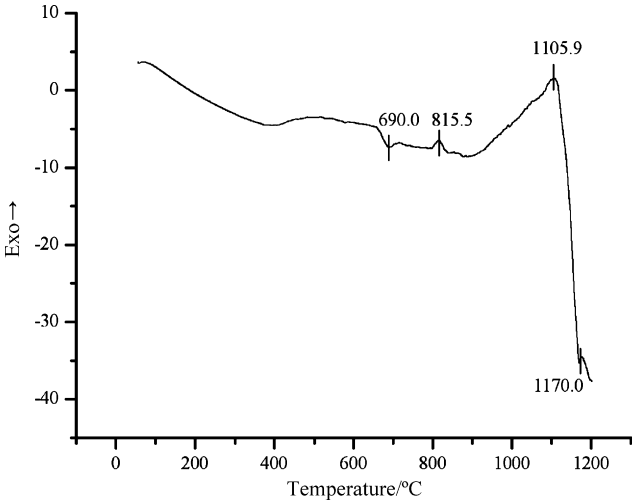

Fig. 1. DTA curve of the as-cast parent glass.

using optical microscopy techniques. Optical microscopy investigations were carried out with XJG-05 optical microscopy made in China. The glass-ceramics optical specimens were prepared using standard metallographic techniques followed by chemical etching in a 6 vol.% HF for 10 s. Moreover, some of the non-etched samples were compared with the etched glass-ceramics samples using optical microscopy techniques.

2.5. X-ray diffraction analysis (XRD)

Powder X-ray diffraction investigations are carried out with D/Max-3B diffractometer using Ni-filtered Cu Kα, operated at 30 kV and 30 mA and in the 2θ range from 10° to 75° at the rate of 4° min^{-1}. The crystal phases were identified by comparing the peak intensities and positions with those in the Joint Committee on Powder Diffraction Standards (JCPDS) data files.

3. Experimental results and discussion

3.1. Thermal characterization

The crystallization of the parent glass was investigated by DTA. Fig. 1 reports the DTA plot of a powdered as-cast glass sample. The glass transformation temperature, T_g, occurs at 690 °C while a clear crystallization exo-peak is at 1105.9 °C, suggesting an intensive crystallization process in the 900–1200 °C temperature range. At the 1170 °C there is a melted endothermic peak, and heat treatment experiments proved that the sample have molten completely at 1200 °C.

3.2. The effects of nucleation temperatures on microstructural characteristics

The research reported that the nucleation rate was high in the vicinity of the endothermic peak and recommended a nucleation temperature near the T_g value. For study of the optimum nucleation temperature, the different nucleation temperatures at 650, 697, and 720 °C at the holding time of 2 h followed by the same crystallization temperature of 900 °C for 2 h were investigated. Fig. 2(a)–(c) are representative typical optical micrographs of non-etched the slag-based glass-ceramics samples nucleated at 650, 697, and 720 °C for 2 h followed by crystallization of 900 °C for 2 h. Fig. 3(a)–(c) are representative optical micrographs of etched the slag-based glass-ceramics samples nucleated at 650, 697, and 720 °C for 2 h followed by crystallization of 900 °C for 2 h.

As seen in Figs. 2 and 3, the crystallized glass consists of branch-like crystals uniformly dispersed in the glassy regions. It is clear that the crystals were more dense and finer in the glass-ceramics samples nucleated at 697 °C for 2 h than at 650 and 720 °C for 2 h, which showed that 697 °C was the most close to the optimum nucleation temperature. As seen in Figs. 2(a) and (c) and 3(a) and (c), large crystals of average sizes of 20–30 μm in the samples nucleated at 650 and 720 °C for 2 h, have been formed indicating that surface crystallization is predominant. As seen in Figs. 2(b) and 3(b), crystals of average sizes in the samples nucleated at 697 °C for 2 h decreased to 10–20 μm, although this sample is still far from optimum. The inherent surface crystallization becomes predominant over bulk heterogeneous crystallization at low crystallization temperatures (900 °C) resulting in large crystalline grain sizes. The surface crystallization at low crystallization temperatures (900 °C) was proved by the columnar crystals growing in the unidirectional direction at the border of the glass-ceramics samples nucleated at 650 °C for 2 h followed by crystallization of 900 °C for 2 h, as shown in Fig. 4. In Fig. 4, the arrows point

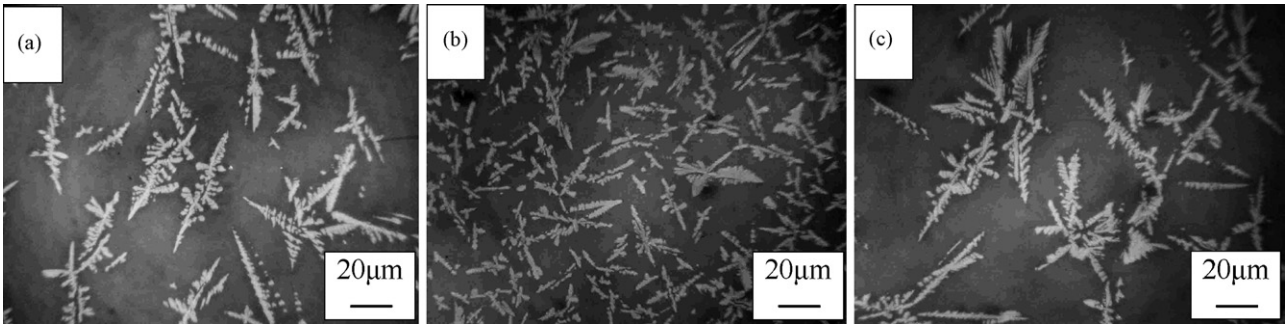

Fig. 2. Representative optical micrographs of non-etched the glass-ceramics samples at different nucleation temperatures for 2 h followed by crystallization of 900 °C for 2 h. (a) 650 °C; (b) 697 °C; (c) 720 °C.

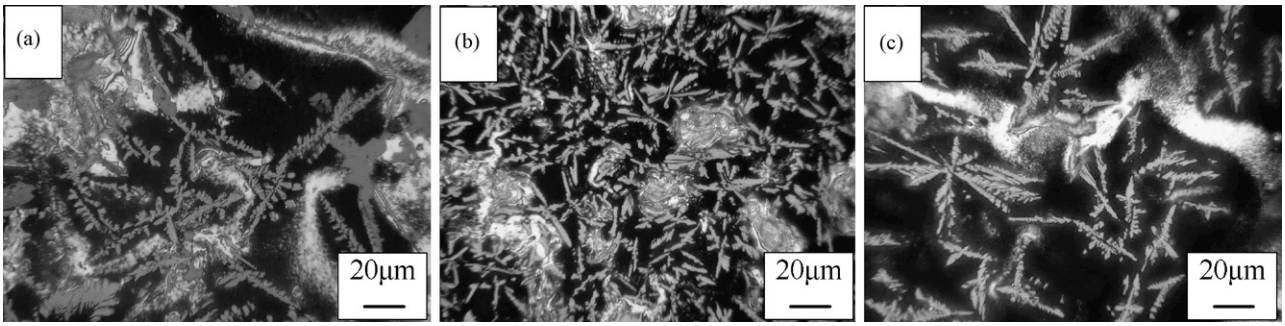

Fig. 3. Representative optical micrographs of etched the glass-ceramics samples at different nucleation temperatures for 2 h followed by crystallization of 900 °C for 2 h. (a) 650 °C; (b) 697 °C; (c) 720 °C.

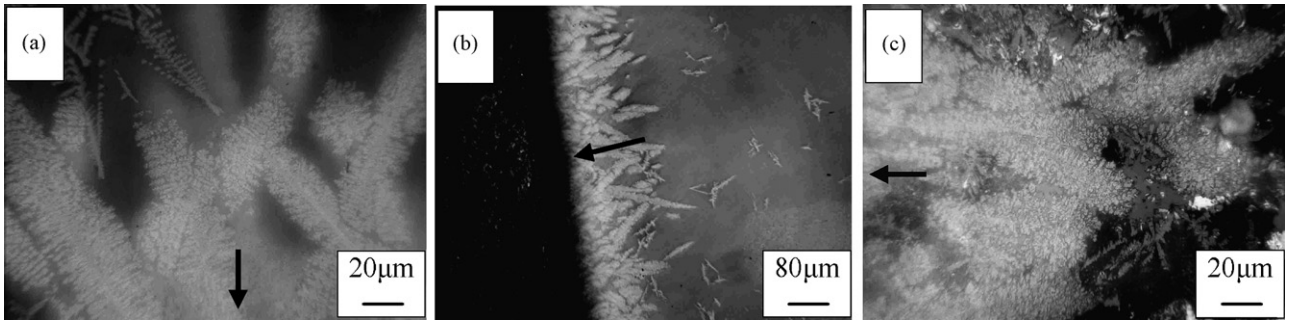

Fig. 4. Optical micrographs of apparent columnar crystals at the border of glass-ceramics samples nucleated at 650 °C for 2 h followed by crystallization of 900 °C for 2 h. (a) Non-etched; (b) non-etched; (c) etched.

to, and are perpendicular to the borders of samples. Further, it can be inferred that due to slower transformation kinetics at 900 °C, some glassy regions might still retain the nucleation ability.

3.3. The effects of crystallization temperatures on microstructural characteristics

For the seek of the optimum crystallization temperatures, the increased crystallization temperatures in the range of 850–1200 °C have been investigated after the samples are nucleated at the optimum nucleation temperatures, 697 °C for 2 h. In the crystallization experiments, surfaces of the crystallized samples show a lot wrinkle and distortion at the crystallization temperature above 1000 °C, and the parent glass samples heated at 1200 °C for 2 h have completely molten. According to Fig. 1, there is a melted endothermic peak near at 1170 °C. Therefore, the following discussed crystallization temperatures of microstructures were lower than 1000 °C.

Fig. 5(a)–(c) are representative optical micrographs of the etched glass-ceramics samples nucleated at 697 °C for 2 h followed by different crystallization at 850, 900, 950 °C for 2 h, respectively. Fig. 5(b) is the same photograph as Fig. 3(b). As seen in Fig. 5(a) and (b), a lot of glass residues have been left in the glass-ceramics body, and a few crystallites were sparsely scattered in glassy regions. As seen in Fig. 5(c), the denser crystallite structures were formed when the crystallization temperatures were up to 950 °C, because the major crystals and the secondary crystals distributed uniformly in glassy regions

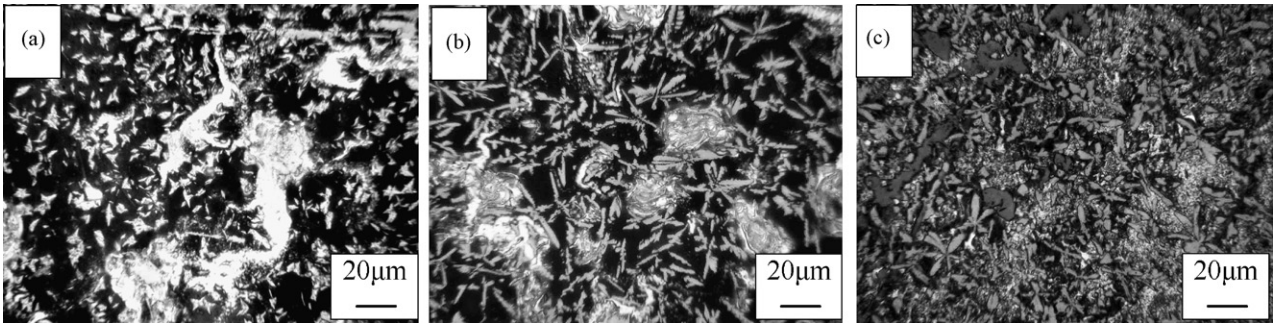

Fig. 5. Representative optical micrographs of etched the glass-ceramics samples nucleated at 697 °C for 2 h followed by different crystallization temperatures for 2 h. (a) 850 °C; (b) 900 °C; (c) 950 °C.

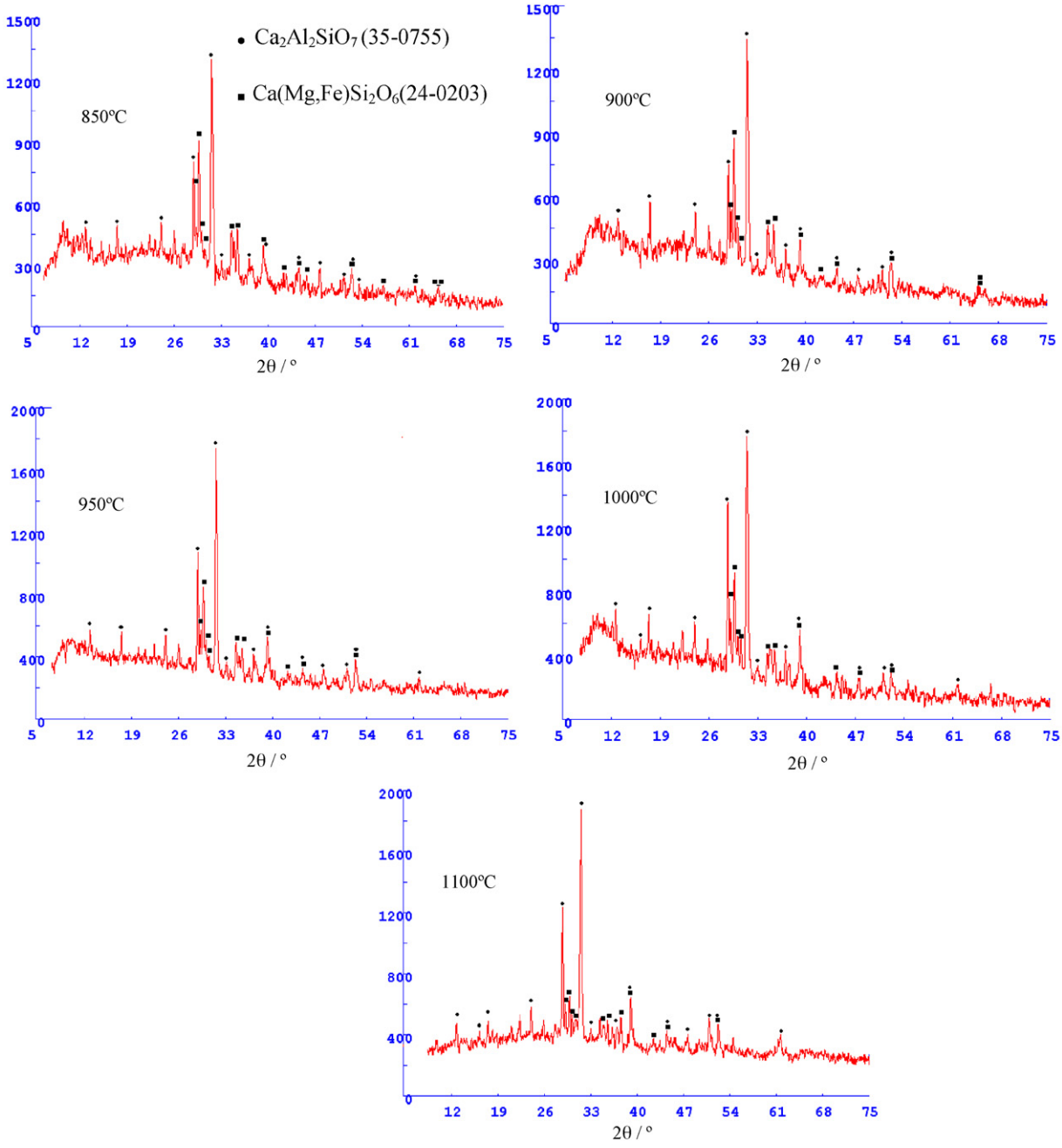

Fig. 6. X-ray diffraction pattern of the glass-ceramics nucleated at the same 697 °C for 2 h followed by different crystallization temperatures respectively for 2 h.

where the proportion of crystal phase increased greatly and the residual glass phase nearly disappeared. The sizes of crystals in Fig. 5(c) are 10–20 μm.

3.4. Crystallizing phases

Fig. 6 shows the result of XRD analysis for the glass-ceramic sample nucleated at 697 °C for 2 h followed by different crystallization temperatures, respectively. It can be seen from Fig. 6 that the glass-ceramics after heat treatment has crystalline phases. The major phase of the glass-ceramics is gehlenite ($Ca_2Al_2SiO_7$) that belongs to the melilite group, and the secondary phase of the glass-ceramics is augite [$Ca(Fe,Mg)Si_2O_6$]. As shown in Fig. 6, with the increase of crystallization temperature from 850 to 1100 °C, the XRD peak intensity of gehlenite increases from 1300 to 2000, however, the XRD peak intensity of augite decreases from 1000 to 700. The change of amount of the two major phases is caused by the reason that augite is transformed into gehlenite at the higher crystallization temperatures in the slag-based glass-ceramics, as reported by M.L. Öveçoğlu [17].

4. Conclusion

The study highlighted the feasibility of recycling red mud and fly ash in the aluminium industries with producing glasses

and glass-ceramics techniques. The red mud is CaO-rich slag from sintering process of Al_2O_3 production. The fly ash, a convenient SiO_2-rich, and Al_2O_3-rich solid waste directly collected from electrostatic precipitator in the coal-combustion power plant, is another main raw material. The glass-ceramic of $CaO–SiO_2–Al_2O_3$ system mostly made from the red mud and fly ash has been developed successfully. The results show that the total amount of both the industrial solid wastes of the red mud and fly ash is up to 85 wt%, which promises less raw materials cost, prominent economic benefits, and environmental benefits.

The parent glass can be vetrificated into crystalline phase after heat treatment, and the denser grain structure can be obtained by a suitable two-stage nucleation–crystallization process, nucleation at 697 °C for 2 h, followed by crystallization temperatures up to 950 °C. With the increase of crystallization temperature from 850 to 1100 °C, the amounts of two major crystalline phases have changed, and the augite transformed into gehlenite at the higher crystallization temperatures in the red mud based glass-ceramics.

Acknowledgments

This research is supported by post doctoral research fund of Shandong Aluminium Co. Ltd.

References

[1] A. Agrawal, K.K. Sahu, B.D. Pandy, Solid waste management in non-ferrous industries in India, Resour. Conserv. Recycl. 42 (2004) 99–120.
[2] N. Yalçın, V. Sevinç, Utilization of bauxite waste in ceramic glazes, Ceram. Int. 26 (2000) 485–493.
[3] C. Liao, H. Lu, D. Qiu, X. Xu, Recovering valuable metals from red mud generation during alumina production, Light Met. 41 (10) (2003) 18–22 (in Chinese).
[4] M. Singh, S.N. Upadhayay, P.M. Prasad, Preparation of special cements from red mud, Waste Manage. 8 (1996) 665–670.
[5] V.M. Sglavo, R. Campostrini, S. Maurina, G. Carturan, M. Monagheddu, G. Budroni, G. Cocco, Bauxite 'red mud' in the ceramic industry. Part I. Thermal behaviour, J. Eur. Ceram. Soc. 20 (2000) 235–244.
[6] E. Şayan, M. Bayramoğlu, Statistical modeling of sulfuric acid leaching of TiO_2 from red mud, Hydrometallurgy 57 (2000) 181–186.
[7] M. Wang, J. Yang, J. Qi, Making unburned and non-autoclaved brick using industrial waste residue, New Build. Mater. 30 (12) (2004) 18–21 (in Chinese).
[8] J. Qi, J. Yang, M. Wang, Experiment research on road base material of red mud, J. Highw. Transport. Res. Dev. 22 (6) (2005) 30–33 (in Chinese).
[9] J.A. Topping, The fabrication of glass-ceramic materials based on blast furnace slag—a review, J. Can. Ceram. Soc. 45 (1976) 63–67.
[10] G. Agarwal, R.F. Speyer, Devitrifying cupola slag for use in abrasive products, JOM 44 (3) (1992) 32–37.
[11] G.A. Khater, The use of Saudi slag production of glass-ceramic materials, Ceram. Int. 18 (1) (2002) 59–67.
[12] H. Endo, Y. Nagayoshi, K. Suzuki, Production of glass ceramics from sewage sludge, Water Sci. Technol. 36 (11) (1997) 235–241.
[13] M. Alonso, E. Sainz, F.A. Lopez, Preparation of glass-forming materials from granulated blast furnace slag, Metall. Mater. Transact. B 27B (1996) 801–809.
[14] M. Erol, S. Küçükbayrak, A. Ersoy-Meriçboyu, M.L. Öveçoğlu, Crystallization behavior of glasses produced from fly ash, J. Eur. Ceram. Soc. 21 (2001) 2835–2841.
[15] A. Karamanov, M. Pelino, M. Salvo, I. Metekovits, Sintered glass-ceramics from incinerator fly ashes. Part II. The influence of the particle size and heat-treatment on the properties, J. Eur. Ceram. Soc. 23 (2003) 1609–1615.
[16] Y.J. Park, S.O. Moon, J. Heo, Crystalline phase control of glass ceramics obtained from sewage sludge fly ash, Ceram. Int. 29 (2003) 223–227.
[17] M.L. Öveçoğlu, Microstructural characterization and physical properties of a slag-based glass-ceramic crystallized at 950 and 1100 °C, J. Eur. Ceram. Soc. 18 (1998) 161–168.